



NIH PUBLIC ACCESS

Author Manuscript

*Cell Cycle*. Author manuscript; available in PMC 2010 March 1.

Published in final edited form as:

*Cell Cycle*. 2009 October 1; 8(19): 3133–3148.

## Temporal differences in DNA replication during the S phase using single fiber analysis of normal human fibroblasts and glioblastoma T98G cells

Rebecca A. Frum, PhD<sup>1</sup>, Zakaria S. Khondker<sup>2</sup>, and David G. Kaufman, MD, PhD<sup>1,\*</sup><sup>1</sup>Department of Pathology and Laboratory Medicine, School of Medicine, University of North Carolina at Chapel Hill, Chapel Hill, NC 27599-7525<sup>2</sup>Department of Biostatistics, School of Public Health, University of North Carolina at Chapel Hill, Chapel Hill, NC 27599-7525

### Abstract

We have recently shown that replication forks pause near origins in normal human fibroblasts (NHF1-hTERT) but not glioblastoma T98G cells. This observation led us to question whether other differences in the replication program may exist between these cell types that may relate to their genetic integrity. To identify differences, we detected immunofluorescently the sequential incorporation of the nucleotide analogs IdU and CldU into replicating DNA at the start of every hour of a synchronized S phase. We then characterized the patterns of labeled replicating DNA tracks and quantified the percentages and lengths of the tracks found at these hourly intervals. From the directionality of labeling in single extended replicating DNA fibers, tracks were categorized as single bidirectional origins, unidirectional elongations, clusters of origins firing in tandem, or merging forks (terminations). Our analysis showed that the start of S phase is enriched in single bidirectional origins in NHF1-hTERT cells, followed by an increase in clustering during mid S phase and an increase in merging forks during late S phase. Early S phase in T98G cells also largely consisted of single bidirectional origin initiations; however, an increase in clustering was delayed until an hour later, and clusters were shorter in mid/late S phase than in NHF1-hTERT cells. The spike in merging forks also did not occur until an hour later in T98G cells. Our observations suggest models to explain the temporal replication of single and clustered origins, and suggest differences in the replication program in a normal and cancer cell line.

### Keywords

DNA replication; S phase; origins; clusters; merging forks; fiber spreading; normal cells; cancer cells

### Introduction

Replication of DNA is thought to occur on or in association with nuclear matrix, an assembly of incompletely defined nuclear proteins.<sup>1</sup> It is reported that DNA is attached to the matrix through matrix attachment regions (MARS)<sup>2</sup> which are thought to be located near origins.<sup>3-8</sup> Attachment of the DNA to the matrix is reported to organize the formation of loops of DNA

\*Corresponding Author: David G. Kaufman, Department of Pathology and Laboratory Medicine, School of Medicine, CB# 7525, University of North Carolina at Chapel Hill, Chapel Hill, NC 27599-7525; 919-966-1396; [uncdgc@med.unc.edu](mailto:uncdgc@med.unc.edu)

Rebecca A. Frum, PhD, [rebecca\\_frum@med.unc.edu](mailto:rebecca_frum@med.unc.edu); Zakaria S. Khondker, [zkhondke@bios.unc.edu](mailto:zkhondke@bios.unc.edu); David G. Kaufman, MD, PhD, [uncdgc@med.unc.edu](mailto:uncdgc@med.unc.edu)

in units ranging in size between 50-200 kb.<sup>3,9,10</sup> The unit of replication, the replicon, has been reported to be of comparable size, between 75-175 kb.<sup>11</sup> The proteins responsible for DNA replication are thought to assemble at the matrix in replication factories or foci.<sup>12-17</sup> It has been suggested that DNA traverses through the factories at the matrix during replication.<sup>1,10,18,19</sup> The assembly of replication factories in the nucleus is very dynamic and details are still being understood. After replication of the DNA in each region of the nucleus, the factories appear to relocate to other parts of the nucleus to replicate other regions of the genome. Chromosomes occupy distinct territories within the nucleus during interphase, and segments of the chromosomes are aligned within these territories by their alternating R and G bands. R and G bands are reported to be organized so that R bands are facing the interior of the nucleus while G bands are located toward the nuclear and nucleolar peripheries.<sup>11</sup> R bands are GC-rich, replicate in the first few hours of S phase and have a high concentration of genes that are transcriptionally active.<sup>20-25</sup> In contrast, G bands typically are AT-rich, replicate later and are gene-poor.<sup>20,22-27</sup> Correspondingly, replication in early S phase appears to occur at multiple sites toward the center of the nucleus, while replication late in S phase tends to be located toward the nuclear periphery.

DNA replication has been visualized at the level of individual DNA fibers using DNA fiber analysis or DNA combing. Initially, this was done with pulses of tritiated thymidine with different specific activities to yield autoradiographic tracks of higher and lower labeling intensity to distinguish the direction of replication.<sup>28</sup> More recent studies have used sequential incorporation of nucleotide analogs iododeoxyuridine (IdU) and chlorodeoxyuridine (CldU), which are detected using specific antibodies linked to secondary antibodies labeled with different colors.<sup>29,30</sup> This labeling strategy leads to different color patterns of labeling which enables visualization of the direction of fork movement.

Fiber analysis has been used to show different aspects of DNA replication, such as rate of fork elongation, and spacing of initiation events and origin choice in mammalian cells. Daboussi et al have used fiber spreading to show that the rate of fork elongation is approximately 1 kb/min in hamster cells.<sup>31</sup> We have found the rate of replication in NHF1-hTERT and T98G cells to range between 1-2 kb/min.<sup>32</sup> In addition, Lebofsky et al have used DNA combing to study origin interference and the spacing between initiation events.<sup>33</sup> Work by Courbet et al has shown that slower rates of DNA replication induced during treatment with aphidicolin at a concentration of 75 ng/ml. leads to the mobilization of latent origins in Chinese hamster fibroblast 471 cells.<sup>34</sup> DNA fiber spreading has also been used to show differences in replication between normal and cancer cells. Using pulse-labeling with <sup>3</sup>H-thymidine and DNA fiber spreads, Martin and Oppenheim showed that the average replicon size of SV40-transformed Chinese hamster lung cells (~31 microns) was significantly less than that of the non-transformed cells (~44 microns).<sup>35</sup> The same investigators also showed that there are more DNA initiation points per unit length DNA in SV40-transformed BALB/c 3T3 cells than in the non-transformed cells.

As with other phases of the cell cycle, replication in S phase occurs in an ordered temporal manner. Jackson and Pombo have shown that regions of the nucleus that replicate early show reproducible patterns of BrdU incorporation in subsequent cell cycles.<sup>30</sup> Other work has demonstrated a reproducible order of gene replication and agreement with identification of very early replicating regions.<sup>21,36-38</sup> Although differences have been reported,<sup>39</sup> it has also been demonstrated that the patterns of nuclear localization of BrdU incorporation at every hour throughout S phase are similar in normal, immortal and cancer cell types,<sup>40</sup> as well as at different developmental stages in mouse cells.<sup>41</sup> Although these studies suggest that the nuclear structure may be conserved in normal and cancer cells, there may be differences between DNA replication in normal cells and cancer cells that could not be detected at the resolution of replication in their studies. It is plausible that unrecognized aberrations from the normal

replication program may contribute to oncogenesis. For example, cells with genetic defects as found in cancer may accomplish the temporal progression through S phase differently. There may be cellular differences between normal and cancer cells, such as fork speed, nucleotide pools, or checkpoint function, that affect initiation of origins, elongation, clustering or termination of forks. These potentially different properties of cancer cells may deregulate DNA replication and contribute to genetic instability.

In the current study, we used fiber analysis to observe how replication progresses throughout 7 hours of the S phase in normal human fibroblasts, and whether these processes differ in T98G cancer cells. The fiber extension technique used enabled us to examine DNA replication throughout S phase at the level of individual fibers, a higher resolution than used in many previous studies, and analyze replication as patterns of sequential DNA precursor incorporation in the nucleus at every hour throughout S phase.

## Results

### Characterization of labeled replication patterns at every hour throughout S phase in normal human fibroblasts (NHF1-hTERT) and glioblastoma (T98G) cells

To understand how replication normally progresses through S phase and whether these normal processes may be deregulated in cancer cells, we synchronized normal human fibroblasts (NHF1-hTERT) and human glioblastoma (T98G) cells to G<sub>0</sub> followed by release into the cell cycle in the presence of aphidicolin to allow cells to accumulate in early S phase. Aphidicolin was removed after 24 hrs and after a 15 min recovery time, the cells were allowed to progress synchronously throughout 7 hours of S phase. At the start of every hour, cells were labeled with the deoxy-nucleotide analog IdU for 10 min, followed sequentially by labeling with a second analog, CldU, for 20 min. After labeling, the cells were collected, and DNA fiber spreads were prepared. In this technique, cells are spread onto a tilted glass slide and are lysed. DNA fibers are aligned and extended on the slide by the gravitational movement of the lysis buffer. Incorporated IdU (detected with an antibody tagged in red) and CldU (detected with an antibody tagged in green) were visualized using a confocal microscope. The patterns of linked red and green labeling produced by incorporation of IdU and CldU indicate the type of replication occurring at that particular site. For example, since replication forks are thought to progress bidirectionally from origins, a red track (first pulse, IdU) flanked on both sides by green (second pulse, CldU) indicates the presence of an origin at the center of the red track activated during the first pulse, with forks proceeding bidirectionally during the second pulse and visualized in green. Sites of unidirectional fork elongation are detected by a single joined red and green track. Merging of replicons (termination) is detected by 2 red tracks joined by a central green track, since this pattern can only be made by forks from 2 different replicons (red tracks) merging and terminating during the second (green) pulse. Likewise, origins firing in tandem were defined in this study as clusters of at least 2 red and 2 green tracks merged into a single labeled unit of replicating DNA. Although red-only and green-only tracks can also be detected, we only included labeled tracks containing both red and green to ensure the replicating DNA was active through the first and second pulses. The different types of replication events revealed by continuously stained patterns of incorporation of IdU and CldU in replicating DNA were quantified and assigned to the categories of single bidirectional origins, unidirectional elongations, clusters of origins activated in tandem, or merging forks (terminations). The lengths of the labeled red and green tracks were measured and recorded for each labeling category at every hour of S phase.

We chose to score labeled fibers only where labeling was continuous to maximize objective identification and reproducible classification of the different replication structures that we scored. We did not make judgments about whether labeled tracks separated by gaps were connected to minimize subjectivity in our scoring. Thus, in this study, labeling patterns with

red-green tracks diverging from a central unlabeled gap were scored as two elongations even though for some it was likely that these were bidirectional replication origins. Those criteria almost certainly cause us to choose not to score some origins. Similarly we did not attempt to resolve whether multiple labeling tracks along a fiber represented a cluster. For this study, clusters were only scored when the labeling between origins had been completed; this approach almost certainly generates a lower score of clusters than would other labeling schemes. More clusters would have been found had we used a longer labeling interval, but then other labeling patterns would have been more difficult to distinguish. By using well-defined criteria for scoring replication figures we expected to improve the reproducibility of our data and to increase the likelihood that we could detect small differences in labeling patterns between time intervals or between normal and cancer cells.

### **Synchronous progression of NHF1-hTERT and T98G cells throughout S phase**

We first confirmed that the NHF1-hTERT and T98G cells were progressing through S phase at similar rates so that the distributions of labeled tracks at each hour would correspond to a comparable stage of the S phase for the two cell lines. Since only actively replicating DNA is detected in the fiber analysis, we compared the percentages of IdU-positive (replicating) NHF1-hTERT and T98G cells in early, mid and late S phase. For our flow cytometric analysis, we labeled the normal and cancer cells with IdU for 10 min at the start of the first, fourth and seventh hours of their synchronous progression through S phase to represent time points during early, mid and late S phase. Then for each flow profile we distinguished cells in early, mid and late S phase compartments and determined the percent of the replicating labeled cells that fell into each of these three bins. We compared the percents of labeled replicating cells in each of the three bins, excluding the unlabeled G<sub>0</sub>/G<sub>1</sub> and G<sub>2</sub>/M fractions, since these corresponded to the labeled replicating DNA that we analyzed in the extended labeled DNA fibers. Our flow cytometry analysis showed that for all three S phase time-points the normal and cancer cells had similar distributions of cells in the early, mid and late S phase bins.

This data indicated to us that replicating NHF1-hTERT and T98G cells were progressing through the S phase at the same rate. It is indeed possible that there are sub-populations with different rates of replication in the cancer cell line, but if such sub-populations are present they represent a sufficiently small proportion of the total population that they do not alter the flow profile enough to produce a detectable difference. Since the fibers we score are representative of the labeled populations seen by flow cytometry the differences we observed between the normal and cancer cells at each hour are due to differences in the replication program at that hour, and not to the presence of a minor sub-population with an atypical program of replication.

Flow cytometric analysis of NHF1-hTERT and T98G cells is shown in Figure 1. Although NHF1-hTERT cells are diploid and T98G cells are hyperpentaploid, both cell lines progress through S phase by doubling their genomic content at a similar rate throughout the 7 hour interval analyzed in this study. Therefore, the subsequent analysis of the distributions and lengths of the fibers at each hour of S phase corresponds to comparable stages of S phase completion in the two cell lines.

### **Scoring of labeled DNA fibers**

We next counted and assigned the labeled tracks produced at the start of each hour into the categories of single bidirectional origins, unidirectional elongating forks, clusters and merging forks (terminations). Figure 2 shows images of the typical replication patterns seen in each hour of the S phase for NHF1-hTERT cells. Examples of fibers that were and were not included in the analysis are shown by block arrows or small arrows, respectively. In Figure 2, we show unprocessed images of the actual fibers that were scored in the analysis. We chose not to subtract background staining or enhance the appearance of the images so that investigators

who repeat this study or use our approach will have a realistic example of the appearance of fibers. Although the fibers are not always evenly aligned, the staining quality and continuity on the fibers in the images was clear enough to identify patterns and measure lengths of labeled fibers.

In Figure 2 we illustrate the criteria employed for selecting fibers to be used in the study and we show overlapping fibers or inadequately stained fibers that could not be scored to explain the criteria we used for eliminating these fibers. We have chosen to emphasize criteria of continuous labeling to maximize the objective identification and reproducible classification of the different structures that we scored. That this approach was successful can be seen from the statistical analysis of the color pattern distributions between replicates of NHF1-hTERT cells and replicates of T98G cells. Our analysis shows that replicates are statistically the same for both cell lines (Fig. 2b). This data shows that not only are the images of a high enough quality to enable statistical reproducibility between repeats, but that our criteria for scoring the coded fibers is consistent enough to produce statistical similarity between repeats.

All of the identifiable fibers on each slide were included for the analysis. We divided the labeled fibers at each hour into the 4 categories for both cell lines to compare their relative percentages and the lengths of the labeled tracks produced during the 30 min of labeling. A statistical analysis was performed on two pooled replicates of NHF1-hTERT and two pooled replicates of T98G to increase the number of fibers in each category for the analysis.

### The temporal replication program in NHF1-hTERT cells

The results in Fig. 3a and Table 1 show that in NHF1-hTERT cells, a large proportion (~32%) of replication events during the 1<sup>st</sup> hour of S phase was single bidirectional origins. During the 1<sup>st</sup> hr, over half (59%) of the total replication occurring was as unidirectional elongations for this cell line (Fig 3b and Table 1). Approximately 6% of replication events occurring during the 1<sup>st</sup> hr was in clusters (Figure 3c and Table 1), and less than 4% of the replication was visualized as merging (terminating) forks (Figure 3d and Table 1). This data shows that a large proportion of replication in early S phase begins largely at single, non-clustered sites in NHF1-hTERT cells.

During the 2<sup>nd</sup> hr, the percent distribution of single bidirectional origins decreased with significantly from 32% in the first hour down to 8% of the scored replication events (Figure 3a, Table 1 and Table 2). A comparison of the percent distributions of origins at the second hr with later timepoints showed no statistical difference, suggesting that enrichment in single bidirectional origins is restricted to the first hour of S phase (Supplemental Table 1). The majority of replication occurred during the second hr as unidirectional elongations (80%) (Figure 3b and Table 1), which was a significant increase from the percent of unidirectional forks present during the first hour (Table 2). This increase in unidirectional elongations may reflect replication forks proceeding from origins initiated in the previous hour. The percent of clusters began to increase from ~6% in the preceding hours to ~11% during the 3<sup>rd</sup> hr (Figure 3c and Table 1 and Supplemental Table 1), and the presence of clusters increased significantly by the start of the 4<sup>th</sup> hour (~20%) (Table 2). Clusters persisted through the 5<sup>th</sup> hr, reaching a peak during this time at 24% (Figure 3c and Table 1). There were significantly more clusters during the 4<sup>th</sup>-6<sup>th</sup> hours of mid S phase than the first two hours of early S phase, suggesting that replication of clusters is a feature of mid to late replication rather than early S phase (Supplemental Table 1). Clusters decreased significantly from this peak to ~13% by the start of the 6<sup>th</sup> hr and comprised a statistically smaller percent of replication events for the rest of S phase compared to mid S phase (Figure 3c, Table 1 and Supplemental Table 1). We also found the proportion of merging (terminating) forks rose throughout S phase (Figure 3d) but there was no statistical difference between hours during the first three hours of S phase (Supplemental Table 1). The increase in terminating forks reached statistical significance by

the 4<sup>th</sup> hr (Table 2) and reached a peak at ~24% of scored events during the 6<sup>th</sup> hr (Figure 3d and Table 1). This peak was statistically significant from the percent of merging (terminating) forks present at any of the preceding times (Supplemental Table 1), and dropped significantly during the following hour (Table 2). This suggests that merging forks accumulate and are resolved during late S phase. Our data suggests that the predominant feature distinguishing early S phase is the replication of single non-clustered origins, while mid S phase is marked by the emergence of replication of tandemly-firing origins, and late S phase is enriched in merging (terminating) forks.

### The temporal replication program in T98G cells and comparison with NHF1-hTERT cells

Similar to NHF1-hTERT cells, we found that replication in T98G cells begins with enrichment of replication at single origins. Single origins comprised 34% of replication occurring during the first hour in T98G cells (Figure 3a and Table 1), which was statistically similar to NHF1-hTERT cells (Table 1). A statistical analysis comparing the percent of single origins in the 1<sup>st</sup> hour of T98G cells with other times of S phase shows there are significantly more origins firing during the 1<sup>st</sup> hour than at any other time in this cell line (Supplemental Table 1). This suggests that similar to NHF1-hTERT cells, the 1<sup>st</sup> hour of S phase in T98G cells is distinguished from the rest of S phase by an enrichment in single bidirectional origins. We also found that during the 1<sup>st</sup> hr, unidirectional elongations comprised 59% of the labeled tracks, while clusters were 5% of the early replicating DNA and merging forks (terminations) were ~2% of the scored fibers (Figure 3b, 3c and 3d and Table 1). There were no statistical differences in the percent distributions of any of the categories between NHF1-hTERT and T98G cells during the first hour of S phase (Table 1), suggesting that NHF1-hTERT and T98G cells may rely on similar strategies for initiating replication at the start of S phase. Also similar to NHF1-hTERT cells, we found a statistically significant decrease in the percent of single origins from the 1<sup>st</sup> to the 2<sup>nd</sup> hour in T98G cells (Table 2). However, the percent of single bidirectional origins decreased to a lesser degree in the T98G cells during the 2<sup>nd</sup> hour compared to NHF1-hTERT cells (Table 1). Approximately 17% of the scored replication events were single bidirectional origins at the start of the 2<sup>nd</sup> hour in T98G while these origins comprised only 8% of labeled fibers during this time in NHF1-hTERT cells (Table 1). This difference between the two cell-types is statistically significant (Table 1). This suggests that T98G cells may depend on more origin initiations in early S phase to replicate their genome, which may lead to differences in their replication program as S phase advances. As was found for the similar time intervals in NHF1-hTERT cells, we found a statistically significant increase in the percent of unidirectional elongations in T98G cells at the start of the 2<sup>nd</sup> hour compared to the 1<sup>st</sup> hour (Table 2). This suggests that similar to the normal cell line, the increase in unidirectional forks during the 2<sup>nd</sup> hour in T98G cells may be reflective of ongoing forks produced by the origins that fired during the preceding hr. However, whereas the percent of unidirectional forks differed significantly between subsequent hours for the majority of S phase in NHF1-hTERT cells, after the 2<sup>nd</sup> hour T98G cells maintained a statistically similar percent of unidirectional elongations between subsequent hours for the remainder of S phase (Supplemental Table 1). We also found that an increase in the clustering of tandemly firing origins did not achieve a level of significance in T98G cells until the 5<sup>th</sup> hour, an hour later than was found in NHF1-hTERT cells (Figure 3c and Table 2). This delay in the emergence of clusters in T98G cells created a statistically significant difference in the presence of clusters during the 4<sup>th</sup> hours in NHF1-hTERT and T98G cells (Table 1). However, the presence of clusters peaked at the same time in both NHF1-hTERT and T98G cells during the 5<sup>th</sup> hour (Figure 3c and Table 1). Similar to the hour delay that we observe in T98G cells for the increase in clustering, we also found an hour delay in the emergence of a spike in merging (terminating) forks in T98G cells compared to NHF1-hTERT cells (Figure 3d). Whereas the percent of merging forks peaks during the 6<sup>th</sup> hour of late S phase in the normal cell line, a spike in the appearance of these merging forks does not occur until the 7<sup>th</sup> hour in T98G cells (Figure 3d). These data suggest that while NHF1-

hTERT and T98G cells follow a similar strategy for enriching replication in early S phase with single bidirectional origins, clusters of tandemly-firing origins in mid S phase, and merging forks (terminations) in late S phase, though differences exist in the timing or degree to which these strategies are utilized for replicating the DNA throughout S phase by these cell lines.

### **Comparison of lengths of replication tracks throughout S phase in NHF1-hTERT and T98G cells**

We next performed a statistical analysis on the total combined lengths of red and green tracks for the same fibers categorized as origins, elongations, clusters and merging forks (terminations) analyzed above. The results in Figure 4 show the average lengths of these replication types by hour and category, converted to kilobases (kb). With few exceptions, the average length of replication tracks was shorter in T98G cells at each hour and for each category than was found in NHF1-hTERT cells (Table 3 and 4). The shorter lengths were found to be statistically significant only during mid to late S phase for unidirectional elongations in the 3<sup>rd</sup> and 6<sup>th</sup> hours and clusters during the 4<sup>th</sup>, 5<sup>th</sup> and 6<sup>th</sup> hours (Table 3). The exceptions where lengths of replication tracks appeared to be longer in T98G cells (although not rising to statistical significance) included single bidirectional origins, clusters and merging (terminating) forks in the 1<sup>st</sup> hour as well as in clusters in the 7<sup>th</sup> hour and terminations in the 5<sup>th</sup> and 7<sup>th</sup> hours (Figure 4 and Table 3). Replication tracks generated during the 30 min total pulse were found to range in size from the shortest (29-33 kb) in both cell lines at unidirectional elongations in early S phase to the longest (167-193 kb in NHF1-hTERT during mid to late S phase, and 136-193 kb during late S phase in T98G) at clusters (Figure 4). We observed that the average length of all tracks steadily increased through the 6<sup>th</sup> hour in NHF1-hTERT cells, then slightly decreased by the 7<sup>th</sup> hour, while the average length of replication tracks produced during the 30 min pulse did not greatly increase until the 7<sup>th</sup> hour in T98G cells (Table 4b). Throughout the duration of S phase, the average length of tracks (by hour) combining all categories was longer in NHF1-hTERT cells than T98G cells for all hours except the 1<sup>st</sup> hour (Table 4b) and they were longer as well for all categories (Table 4a). In general, throughout the entire S phase, the overall average track length was found to be approximately 17% shorter in T98G cells compared to NHF1-hTERT.

### **Determination of inter-origin distances in clusters in NHF1-hTERT and T98G cells**

We next performed an analysis to determine the average inter-origin distance in clusters in both NHF1-hTERT and T98G cells. Since the red tracks produced from the first pulse with IdU are likely origins within the clusters, we counted the number of red tracks in a cluster at each hour and divided this averaged number into the average length of clusters (converted to kb as described in Methods) at that hour. We found that although the length of clusters varied by up to 2-fold between different hours within the same cell line or at the same hour between cell lines, the average number of red tracks (origins) was very similar for all time-points and both cell lines (a range of 2.2 to 3.1 in NHF1-hTERT, and 2.3 to 3.1 in T98G) (Table 5). We found for both NHF1-hTERT and T98G cells, there was an average of 2.6 red tracks in a cluster throughout S phase (Table 5). This number was independent of cluster length, suggesting there may be a requirement, perhaps by the replication machinery, for approximately 3 origins to fire during the replication of a cluster (as determined by our labeling protocol). It is possible that the average 2.6 origins firing per cluster, independent of length of the cluster, may represent a unit of replicating DNA, possibly representing loop length or length of epigenetically activated replicating DNA. We found the average inter-origin distance throughout S phase was 57 kb in NHF1-hTERT cells and 48 kb in T98G cells, suggesting there may be additional origins activated in T98G cells (Table 5) to accomplish DNA duplication in the same time interval.

## Discussion

We compared replication dynamics during 7 hourly intervals of S phase in NHF1-hTERT and T98G cells by examining individual replicating DNA fibers. NHF1-hTERT cells and T98G cells were synchronized by confluence arrest or serum starvation, respectively, followed by aphidicolin treatment to enrich the cycling population at the start of S phase. Both cell lines were synchronized to G<sub>0</sub> followed by release into medium containing aphidicolin to enable cells to accumulate synchronously in early S phase; aphidicolin treatment for 24 hours was used to minimize differences in replication dynamics between cell types that could be due to the synchronization method.<sup>32</sup> Although immortalized NHF1-hTERT cells are diploid, and T98G are hyperpentaploid, both cell lines show similar progression in doubling their DNA content through the 7 hour interval, presumably because there are more origins and more active sites of replication in T98G cells. This is in agreement with a previous report demonstrating that there are more DNA initiation sites per unit length of DNA in aneuploid SV40-transformed BALB/c 3T3 cells than in non-transformed BALB/c 3T3 cells.<sup>42</sup>

Despite having achieved rather good synchronization of the cell populations there is still minor variability of the timing of entrance into S phase and the timing when individual origins fire in individual cells. Synchronization of cells with aphidicolin as employed in our studies greatly slows but does not stop replication. We have found that during the 24 hour incubation in aphidicolin during our synchronization protocol, replication progresses equivalent to about 20 min of a normal S phase.<sup>43</sup> While aphidicolin is present and following its removal, origins fire continuously not as a synchronous cohort. In our studies we chose to delay the start of labeling until 15 minutes after the removal of aphidicolin to allow the cells to recover from residual effects of aphidicolin on nucleotide pools and to restore normal rates of replication. For consistency we begin all 7 hourly time-points with this 15 minute interval before we began to label cells with IdU (red) followed by CldU (green). Since we are making comparisons between different replication forms seen at different times in S in the same cells and we compared these events between cells we do not think that the concerns about replication rates or rates of entry of precursors into cells are a concern in these experiments.

Our data suggests that for both NHF1-hTERT and T98G cells, single non-clustered bidirectional origins are most prevalent during the first hour of S phase, and this type of replication event is dramatically reduced for the remainder of the S phase. The decrease in single bidirectional origins is less extensive during the second hour in T98G cells, however, suggesting that there may be a difference in regulation or coordination of origin firing in early S phase of the cancer cell line. This would support previous observations that there is deregulation of origin initiations in cancer cells. Our data also suggests that replication in early S phase may be largely composed of initiations originating from individual sites controlled by single origins without activation of nearby origins in both cell types. The increase in the number of unidirectional elongations that follows in the 2<sup>nd</sup> hour in both NHF1-hTERT and T98G cells may reflect the large percentage of single origins that are active during the first hr of S phase, since the origins firing in the 1<sup>st</sup> hour presumably produce some of the unidirectional forks extending from these origins. We have recently shown that replication forks near single bidirectional origins pause for at least 10 min after an initial 10 min of synthesis at origins that fire during the 1<sup>st</sup> hour of S phase in NHF1-hTERT cells, and that this pausing is absent in the early S phase of T98G cells.<sup>32</sup> It is interesting to note that the total lengths of single bidirectional origin replication tracks labeled for the 30 minute interval in the present study are longer in NHF1-hTERT than T98G at all hours except for the 1<sup>st</sup> hour. This finding is consistent with the pausing of replication near origins that occurs only during the 1<sup>st</sup> hour of S phase in NHF1-hTERT cells but is inoperative in T98G cells. This effect is sufficient to reduce the length of labels fibers at bidirectional origins to be detected.



It was shown previously that multiple origins can fire in tandem clusters at the same time.<sup>30</sup> We have found that replication events occurring in tandemly activated adjacent DNA segments (clusters) were prevalent during the mid to late S phase in NHF1-hTERT cells, and the length of the clusters increased until the 4<sup>th</sup> hour and then reached a plateau. However, an increase in the distribution of clusters during the S phase of T98G cells was not seen until an hour later than in NHF1-hTERT, and lengths of clusters did not increase until late S phase. The lengths of clusters in T98G cells were statistically shorter than NHF1-hTERT during late S phase (4<sup>th</sup>, 5<sup>th</sup> and 6<sup>th</sup> hours). Although our method of fiber spreading enabled us to discern increases in the presence of clusters as S phase progressed, the actual percent distribution of clusters may be underestimated in our analysis since their longer length may have caused breakage or tangling with other fibers which might have made it difficult to measure them accurately. However, analysis of the data clearly shows that there is a trend of clustering that is most pronounced during mid-to-late or late S phase as opposed to early S phase. Our data also demonstrates that there is a larger percent distribution of unidirectional elongations during the 4<sup>th</sup>-6<sup>th</sup> hours of S phase in T98G cells compared to NHF1-hTERT cells. The greater distribution of individual forks in mid to late S phase of T98G cells may indicate more individual sites of active replication along the chromosomes in this cell line during this time, which may explain or reflect less clustering and the shorter lengths of the clusters during the 3<sup>rd</sup>-6<sup>th</sup> hours in T98G cells.

Another difference in replication between the two cell types was found during late S phase, when the percent distribution of merging forks (terminations) increases in NHF1-hTERT cells during the 5<sup>th</sup> hour and peaks during the 6<sup>th</sup> hour, while the distribution of merging forks decreases during these times in T98G and peaks later during the 7<sup>th</sup> hour. Although the red-green-red patterns we scored indicate areas of merging (terminating) forks, and an increase in these patterns does not occur in T98G cells until later in S phase than found in NHF1-hTERT, there may be other ways that replication at certain sites gets completed in late S phase other than by that indicated by this specific labeling pattern. The red-green-red pattern shows the simultaneous meeting of two replication forks, but not all terminations may be visualized as two forks simultaneously converging at the same time. For example, one of the converging forks may be delayed or further away from the other converging fork during late S phase of T98G cells, which could explain why there are fewer red-green-red terminating patterns during this time in T98G cells. Alternatively, there may be a shorter distance between merging replicons in late S phase of T98G cells that may result in merging of forks during the first (red) pulse, producing red only tracks, and thereby artificially reducing the percent of terminations in T98G cells visualized as red-green-red tracks. Replication may also be slower in T98G cells, so by the 5<sup>th</sup> and 6<sup>th</sup> hours when terminating forks merge in NHF1-hTERT cells, units of replication may not be ready to terminate in T98G cells until later. The smaller percent distribution of merging forks indicated by the red-green-red pattern in late S phase of T98G cells may not indicate that there are fewer terminations occurring during this time in this cell line but the process and labeling pattern may be different. However, the higher occurrence of merging forks during the 5<sup>th</sup> and 6<sup>th</sup> hours of S phase in NHF1-hTERT than in T98G cells may also suggest that the normal program of replication termination during late S phase is altered in the cancer cell line. Cha et al have shown that terminations accumulate during late S phase.<sup>44</sup> The smaller percent of merging (terminating) forks that we observe during late S phase in T98G cells may play a role in DNA breakage or genomic instability because unresolved terminations may be present at the end of S phase and may persist to be resolved later when the cells are in the G2 phase. Fragile sites, where breakage of DNA occurs with increased frequencies, replicate late in S phase<sup>45-52</sup>, the same time when we find a smaller percentage of terminations in T98G cells than in NHF1. It is plausible that these late-replicating fragile sites may be subjected to breakage due to faulty or delayed termination of replicons. It is conceivable that a faulty program of terminations during late S phase may have led to a higher

rate of breakage of DNA or the persistence of unreplicated regions in the DNA in the late S phase of T98G cells; such processes may have contributed to their abnormal DNA content.

A recent paper by Conti et al addresses replication fork velocities in adjacently-firing origins.<sup>53</sup> These authors report a large heterogeneity in fork velocity, with a mean fork velocity of 1.46 kb/min in primary normal keratinocytes. We report a similar rate in NHF1-hTERT and T98G cells, varying between 1-2 kb/min at different hourly intervals throughout S phase. This rate was calculated from the total length of the tracks with the single red-green pattern produced during 30 min of labeling (not shown), assuming that the majority of these tracks represent continual unidirectional fork movement.

Conti et al<sup>53</sup> and we have both addressed the issue of inter-origin distances in clusters. Clusters have been defined as 2-9 adjacent replicons that are replicated simultaneously because of their close proximity to the replication machinery (foci), within a timeframe of 45-60 min.<sup>30,54,55</sup> Conti et al have also shown the median interorigin distance between adjacently-firing origins as 111 kb in asynchronous primary normal keratinocytes.<sup>53</sup> Here we show an average interorigin distance in clusters for the averaged 7 hours of S phase as 57 kb in NHF1-hTERT cells and 48 kb in T98G cells. These differences in values between the two studies may be explained by different criteria used to evaluate inter-origin distances (i.e, the requirement for a continuously labeled fiber) and the shorter labeling interval used in our study. Conti, et al. aimed to determine fork velocity at adjacent origins, using IdU and CldU, and this required unlabeled space (gaps) between adjacent replicons. To study fork velocity at adjacent origins, fibers were selected based on replication of the adjacent origins not being completed during the 40 min labeling interval, as some of the origins initiated before labeling started, producing unlabeled “gaps” between bidirectional forks, representing origins in the gap, and replication of some adjacent replicons was not completed by the end of the labeling interval. Since labeled forks from adjacent origins in the scored fibers do not always meet during the 40 min labeling interval, these “clusters” of adjacent initiating origins probably represent larger replicons, with the determined mean interorigin distance of 111 kb. In contrast, our inter-origin distances were calculated by tandem origins firing simultaneously in a continually labeled track with no gaps, that was completed within 30 min of labeling. These well may be smaller “clusters” than those evaluated in the Conti et al study, with an average inter-origin distance of 57 kb for the averaged 7 hours of S phase in NHF1-hTERT cells, and 48 kb for the averaged S phase interval in T98G cells. We show that more of these “clusters” of tandemly firing origins accumulate during mid S phase in NHF1-hTERT cells and they are longer in mid S phase than in T98G cells. The results of our study might have been more like those of Conti had we used longer labeling intervals which would have allowed the DNA between more distantly spaced origins to have labeled. In interpreting these cluster results in our study what we may be comparing is a subclass of replicon clusters that are activated simultaneously from origins no further apart than about 50 kb. In this case our results should not be interpreted as reflecting all replication at contiguous clusters of simultaneously replicated replicons. Interestingly, Conti, et al. and we both observe approximately three origins activated per cluster. We found there was an average of 2.6 origins initiated per simultaneously activated cluster regardless of cluster length or cell type. This may reflect a fundamental requirement of replication factories to accomplish the replication of clustered regions of DNA whose adjacent origins are activated in tandem.

Previous studies have shown that replicons that initiate as S phase begins were activated in small clusters.<sup>30,54</sup> In our study, we show that S phase begins largely with the initiation of single bidirectional origins, while replication that occurs during mid to late S phase is largely enriched in clusters of origins that simultaneously fire in tandem producing a continually labeled track during the labeling scheme. We believe the differences of interpretations between those observed in previous studies and those in our study reflect both the different methodologies and objectives in these studies. In operationally defining a “cluster” of replicons

as 2 or more adjacent actively replicating units that merge into a continuously labeled track during the total 30 min labeling time we put a very stringent and more narrow requirement than in past studies where the proximity of labeled replicating tracks even if separated by an unlabeled gaps could be interpreted as clustered synchronously activated replicons on the same fiber. It is likely, therefore, that our approach underestimates the number of adjacent synchronously activated replicons. We did not label fibers with a general DNA stain and score labeling tracks on the same DNA fiber but separated by unlabeled gaps since the objective of our study was to acquire data that allowed us to distinguish quantitatively differences in patterns of replication at different times in S phase and between normal and malignant cells with minimal subjectivity. We believe that this objective was met well by the methods employed as demonstrated by the statistical analysis of the labeling pattern distributions between replicates of NHF1-hTERT cells and replicates of T98G cells which show that replicates are statistically the same for both cell lines. This data shows that the images we analyzed were of a high enough quality to achieve statistical reproducibility between repeats, and further that our criteria for scoring the coded fibers is sufficiently consistent to validate the statistical similarity of results in repeat experiments. Nonetheless, the lack of a DNA fiber label and our choice not to score apparent clusters separated with unlabeled gaps could also have resulted in an underestimate of the frequency of clustering of origins in our studies. Further, it is entirely possible that if we had chosen longer labeling intervals, more replication would have been recognized as having occurred in clusters even using our definition. However, by using the criteria that clusters be contiguously labeled without gaps, we also more objectively quantify clustering of adjacent replicons, since there is no ambiguity about where or whether origins lie in the gaps between labeled tracks. We recognize that we are assessing only a fraction of potential clusters by the labeling protocol used and the criteria we chose for scoring labeling patterns. We chose our criteria of continuously labeled tracks to optimize the recognition of labeling patterns and facilitate statistical analysis of data sets. Since our objectives in this study were more to characterize differences in replication at successive hours through S phase and to compare a normal and cancer cell line, the more rigid objective criteria were advantageous in reducing noise in our analysis to distinguish what might be small but significant differences.

Our data shows that a large proportion of replication events occurring during early S phase in both NHF1-hTERT and T98G cells are in the form of single bidirectional origins. The distribution of replication events shifts toward more clustering of replication sites during mid S phase in NHF1-hTERT cells; clusters are shorter and occur later in T98G cells than in the normal cells. These observations prompted us to speculate about reasons for the prevalence of single bidirectional origins and shorter clusters in early S phase in both NHF1-hTERT and T98G cells and in T98G cells compared to NHF1-hTERT cells during the middle of S phase. We can envision two different scenarios to explain this data. In Figure 5a, we illustrate one of these hypotheses in which our observations may be explained by a different organization of DNA into loops during early and mid S phase. DNA loops are thought to be created via attachment of the DNA to the nuclear matrix through matrix attachment regions (MARS)<sup>2</sup>; origins of DNA replication are also thought to be located near MARS.<sup>3,9,10</sup> It has been shown that actively transcribed sequences are closely associated with the matrix.<sup>56-62</sup> Since most DNA that is actively transcribed is replicated in the first few hours of S phase<sup>20-25</sup>, this suggests there may be more sites of attachment of DNA to the matrix in early S phase. This may lead to formation of smaller loops than in mid S phase, when replication occurs more frequently in transcriptionally-inactive heterochromatin.<sup>63-66</sup> Models for DNA replication have proposed that after initiation at origins, replication of DNA occurs at the nuclear matrix as DNA is reeled through replication factories associated with the matrix.<sup>1,10,18,19</sup> We hypothesize that if replication occurs by the reeling of DNA loops through the replication machinery, the prevalence of single origins in early S phase and clusters in mid S phase may be determined by differences in loop size and therefore number of origins present in the loops. Since actively transcribed genes are replicated in early S phase, and MARS are generally associated with

actively transcribed DNA, it is possible that there is more extensive attachment of the DNA to the matrix in early replicating DNA; this may create smaller loops by the anchoring of many potential origins to the matrix. As these origins anchoring the ends of the loop would be pulled through the replication machinery at the matrix this could lead to what we visualize as replication of unclustered single bidirectional origins. In contrast, sites of attachment of DNA to the matrix during the middle of S phase may occur less frequently, since DNA that replicates during this time is less transcriptionally active. This organization of the DNA may result in larger loops containing multiple origins. It is possible that when these larger loops are replicated, the licensed origins in the loop may simultaneously be pulled down to assemble at the matrix sites near replication factories (or foci), and thus be activated to fire at the same time. This may lead to the increase of clusters that we observe during the middle of S phase. Our observations support the results of Tomilin et al who reported the presence of mini-foci in early S phase nuclei and suggest that these represent single replicons that may correspond to DNA loop domains.<sup>67</sup> In addition, during *Xenopus* development, an increase in the length of DNA loops is associated with a reduced number of MARS.<sup>68</sup>

Our hypothesis that the length of the labeled tracks may represent the size of the DNA loops, as well as our observation that clusters of shorter length are replicated during mid S phase in cancer cells, is supported by a study by Linskens et al.<sup>69</sup> This group showed that transformed BHK cells have a shorter average DNA loop length than non-transformed cells. In agreement with this study, we have observed shorter clusters during mid S phase of glioblastoma T98G cells than normal NHF1-hTERT cells. Our results in conjunction with the study by Linskens et al. suggest that the shorter clusters during mid S phase in T98G cells may be due to smaller loops in this cancer cell line. Linskens et al speculated that shorter loop size in transformed cells may result in more origins being active, since there would be more attachment to the matrix, and a higher number of matrix-associated origin initiations may lead to deregulated DNA replication.<sup>69</sup>

Our analysis of labeled DNA track lengths has shown that 30 min of labeling produces single bidirectional origins that range in length from 48-107 kb in NHF1-hTERT cells, and 47-80 kb in T98G cells. We have also shown that clusters of tandem replicons range in size in NHF1-hTERT cells from 88- 189 kb and in T98G cells from 93-193 kb. It has been reported previously that DNA loops resulting from the attachment of DNA to the matrix range in size between 50-200 kb.<sup>9</sup> This loop size is comparable to the lengths of the labeled single bidirectional origins and clusters that we found in NHF1-hTERT and T98G cells, which supports our hypothesis that the single origins found in early S phase and the clusters of tandem replicons found in mid S phase may comprise different organization of DNA into loops during early and mid S phase. However, factors that control the occurrence of single or clustered units of replication, and whether loops of different sizes contain single or multiple replicons, have not yet been determined.

In addition to differences in loop size, we hypothesize there may be an alternate explanation for single or clustered origins in early or later S phase. In Figure 5b, we illustrate that it is also possible that these replication patterns may be explained by differences in the status of the chromatin at different times in S phase. Since early replicating DNA is generally transcriptionally active, chromatin in these regions may have more activating epigenetic marks. This property might make the individual origins in these regions more accessible to the nuclear matrix and replication factors, and might lead to the activation of single origins with the most activating of epigenetic marks. In support of this hypothesis, it has been suggested that chromatin remodeling associated with transcription factors may be involved in site-specific origin recognition in eukaryotes.<sup>70</sup> This site-specific origin recognition may be reflected in the high percentage of single bidirectional origins that we observe in early S phase. DNA replicated in the middle of S phase, however, is generally less transcriptionally active with less-activating

epigenetic marks, which may make the selection of replication origins to activate more random. Therefore, replication through such heterochromatin may allow adjacent replication origins to have access to nuclear matrix and replication factors, which would favor simultaneous firing of tandem origins. Support for this hypothesis comes from comparison of the replication timing analysis of early and later replicating regions of the genome. Comparisons between normal human fibroblasts and human lymphoblasts showed the similarities of replication timing of early regions between the two different human cell types<sup>21,36</sup>, while the order of replication of genes that initiate in mid and late S phase is not as reproducible. Differences in replication timing of early or late replicating DNA between cell types may therefore be reflective of different epigenetic markings that result in reproducible firing of single origins in early S phase and the more random selection of origins firing in clusters during later S phase. This model would predict that DNA replicated at later times in S phase may exist in loops the same size as found earlier in S phase, and the firing of tandem origins observed later as replication progresses may reflect differences in chromatin status and the requirement for remodeling. This may be reflected in the small replication foci or factories that are observed during early S phase, which may be sufficient for the replication of single origins during that time, while the larger factories found present later in S phase may be required for the firing of adjacent origins, and leading to the clusters that we observe in mid S phase.<sup>18,19</sup> This hypothesis is further supported by the observation that DNA loop size correlates with the size of replicons.<sup>71-72</sup> It is possible that the individual origin patterns that we observe in early S phase may reflect starting points for replication in dispersed sites on multiple chromosomes, while clustering of tandem-firing origins in mid S phase may suggest more replication localized to one or a few chromosomes at a replication focus in the middle of S phase.

Our observations show and compare properties of replication throughout S phase in a single normal and single cancer cell line. We have categorized the patterns of replication as single bidirectional origins, unidirectional elongations, clusters and merging forks (terminations); however, this is our current definition of what these patterns mean, and our interpretation of how replication proceeds throughout S phase is based on the patterns produced during 10 min of labeling with one analog followed by 20 min with a different analog. It is possible that later studies will show that these patterns indicate replication events other than those we classify in this study; for example, unidirectional elongations visualized in our experiments may represent unidirectional fork movement at an origin rather than distal to an origin (Frum and Kaufman, unpublished observation), or these patterns may represent broken DNA.

In addition to confirming some previous observations on replication, our data suggests there are differences in the replication program as replication proceeds through early, mid and late S phase. We propose that these differences may be explained by the manner in which early or later replicating DNA is organized into loops or by the chromatin status of DNA which may reflect the transcriptional activity of the replicating regions. Our data shows the program of replication in one normal and one cancer cell line, and suggests how replication through S phase differs between them. The differences in replication that we show are applicable to these cell lines; the applicability of these differences to all normal and cancer cell lines remains to be established. However, our studies suggest different strategies for replicating DNA within two different cellular contexts; these differences and their contribution to genetic instability may be investigated in future studies.

## Materials and Methods

### Cell lines and synchronization

Normal human diploid fibroblasts (NHF1-hTERT), derived from neonatal foreskin and immortalized by expression of telomerase reverse transcriptase (hTERT)<sup>73-74</sup> and malignant T98G glioblastoma cells were cultured in minimum essential medium (MEM) (Gibco)

supplemented with 2mM L-glutamine (Gibco) and 10% fetal bovine serum (FBS) (Hyclone Laboratories, Inc.). NHF1-hTERT cells were seeded at  $1 \times 10^6$  cells/100mm plate and were grown to confluence arrest for seven days with media changed on the third and fifth days, followed by replating at 374,000 cells/60mm plate for fiber spreading, or 600,000-800,000 cells/100mm plate for flow cytometry. T98G cells were serum starved for three days in 0.2% FBS followed by release into MEM with 10% FBS. For both cell types, aphidicolin (A.G. Scientific, Inc.) was added to the culture medium at a concentration of 2 $\mu$ g/ml for 24 hr at release from confluence arrest or serum starvation. After 24 hr, aphidicolin was removed using three washes with Hanks' balanced salt solution with calcium (HBSS) (HyClone), and cells were incubated in complete medium for 15 min before labeling. Thereafter, cells were labeled with nucleotide analogs as described below.

### Labeling of cells with thymidine analogs

Actively replicating cells at the start of each hour of S phase (based on time after release from the aphidicolin block) were first labeled with the thymidine analog IdU (50 $\mu$ M) (Sigma) for 10 min, washed three times with HBSS and then labeled with CldU (100 $\mu$ M) (Sigma) for 20 min. IdU and CldU incorporated into replicating DNA were later detected with antibodies that fluoresce red or green, respectively, as described below. Two independent replicate experiments were performed and analyzed for both NHF1-hTERT and T98G cells.

### DNA fiber spreading

Spreads of extended DNA fibers were made as described earlier with modifications.<sup>30,75</sup> After labeling, the cells were trypsinized and resuspended in Phosphate Buffered Saline (PBS) (Sigma) at 200 cells/ $\mu$ l. Two  $\mu$ l of cell suspension was streaked across a silane-coated slide (Sigma-Aldrich) and allowed to air dry almost completely. Eight  $\mu$ l of spreading buffer (0.5% SDS in 200mM Tris-HCl, pH 7.4, 50mM EDTA) was added to the streaked cells. After 10 min, the slides were tilted at 15°, and the buffer was allowed to run down the slide. The resulting DNA spreads were air-dried, fixed in 3:1 methanol/acetic acid, and frozen overnight.

### Immunostaining

Slides were treated with 2.5M HCl for 30 min, washed once in PBS/0.1% Tween 20 and twice in PBS and then exposed to 2% bovine serum albumin in PBS for 40 min. The slides were then incubated with the primary antibody mixture at room temperature in a humid chamber: 1 hour in 1:250 rat anti-bromodeoxyuridine (detects CldU) (OBT0030, Accurate) plus 1:250 mouse anti-bromodeoxyuridine (detects IdU) (Becton Dickinson). After this step, slides were incubated for 10 min in a stringency wash buffer containing 10 mM Tris HCl pH 7.4, 400 mM NaCl, and 0.2% Nonidet 40 (NP40) to eliminate non-specifically bound primary antibodies. Slides were then washed twice in PBS. The slides were then incubated in the secondary antibody mixture in a humid chamber at room temperature: 30 min in 1:250 Alexafluor 488-conjugated chicken anti-rat (Molecular Probes) plus 1:333 Alexafluor 594-conjugated rabbit anti-mouse (Molecular Probes). Slides were washed once in PBS/0.1% Tween 20 followed by two washes in PBS. Before incubation in the third antibody mixture, slides were incubated with 2% Normal Goat Serum (Gibco) in PBS for 15 min to suppress subsequent non-specific binding by goat antibodies. The third antibody mixture was added in a humid chamber at room temperature: 30 min in 1:250 Alexafluor 488-conjugated goat anti-chicken (Molecular Probes) plus 1:333 Alexafluor 594-conjugated goat anti-rabbit (Molecular Probes). The slides were then washed as described following incubation in the secondary antibody mixture. The slides were mounted in antifade (UNC Microscopy Core). Microscopy was carried out using an Olympus FV500 confocal microscope using the sequential scanning mode. Tracks without gaps in staining were measured using Image J software. After staining, slides were assigned a random code number, and the fibers were scored by code number. During data collection, the

analyzer was unaware of the identity of the samples. After collecting the data, the slides were decoded. Further analysis of data was performed after decoding the slides.

### Statistical Analysis

For the analysis of length data, a general linear model was fit using length as response and cell type, hour, and category and all their interactions as predictors, adjusting for replicates. Least squares differences between the mean lengths of cancer cells and normal cells were estimated and corresponding p-values were calculated for each category and hour using t-tests. For the analysis of distribution data, a Poisson regression model was fit using percentage of each replication event compared to all replication events as response and cell type, hour, and category and all their interactions as predictors, adjusting for replicates. Least squares differences between the mean percentages of cancer cells and normal cells were estimated and corresponding p-values were calculated for each category and hour using chi-square tests. Adjustments for multiple testing were done using Sheffe's method for the analysis of length. The statistical method for percentage distribution is less powerful and any adjustment for multiplicity with only two replicates is not viable. The total number of fibers scored for the analyses combining both replicates for NHF1-hTERT cells was: 1<sup>st</sup> hr: 253; 2<sup>nd</sup> hr: 288; 3<sup>rd</sup> hr: 316; 4<sup>th</sup> hr: 316; 5<sup>th</sup> hr: 271; 6<sup>th</sup> hr: 311; 7<sup>th</sup> hr: 251. The total number of fibers analyzed combining both replicates in T98G cells was: 1<sup>st</sup> hr: 459; 2<sup>nd</sup> hr: 390; 3<sup>rd</sup> hr: 338; 4<sup>th</sup> hr: 303; 5<sup>th</sup> hr: 184; 6<sup>th</sup> hr: 250; 7<sup>th</sup> hr: 200.

### Flow cytometry

Cells for flow cytometric analysis were labeled at the start of each time point for 10 min with 50  $\mu$ M IdU. The cells were then trypsinized, collected, washed twice with PBS and fixed in 70% cold ethanol. Staining was performed following a published protocol.<sup>76</sup> Cells were incubated in primary antibody, 1:10 mouse anti-bromodeoxyuridine (Becton Dickinson) to detect IdU, for 30 min, followed by incubation in the secondary antibody, 1:500 goat anti-mouse FITC (Sigma Aldrich), for 30 min in the dark. The cells were run on a CyAn flow cytometer and cell cycle distributions were analyzed using Summit software.

### Supplementary Material

Refer to Web version on PubMed Central for supplementary material.

### Acknowledgments

We thank Dr. Jean Cook for generously providing T98G cells. We also thank Dr. Paul Chastain and Dr. Bruna Brylawski for reading and carefully critiquing the manuscript. This work was supported by a grant from the National Cancer Institute (R01-CA084493) (DGK) and a Postdoctoral Fellowship from the National Institute of Environmental Health Sciences (T32-ES07017) (RAF).

**Supported by:** A research grant from the National Cancer Institute (R01-CA084493) (DGK) and a Postdoctoral Fellowship from the National Institute of Environmental Health Sciences (T32-ES07017) (RAF).

### References

1. Cook P. The nucleoskeleton and the topology of replication. *Cell* 1991;66:627–35. [PubMed: 1652367]
2. Heng H, Goetze S, Ye CJ, Liu G, Stevens JB, Bremer SW, et al. Chromatin loops are selectively anchored using scaffold/matrix-attachment regions. *J Cell Sci* 2004;117:999–1008. [PubMed: 14996931]
3. Vogelstein B, Pardoll DM, Coffey DS. Supercoiled loops and eukaryotic DNA replication. *Cell* 1980;22:79–85. [PubMed: 7428042]
4. Smith H, Puvion E, Buchholtz LA, Berezney R. Spatial distribution of DNA loop attachment and replicational sites in the nuclear matrix. *J Cell Biol* 1984;99:1794–802. [PubMed: 6490720]

5. van der Velden H, van Willigen G, Wetzels RH, Wanka F. Attachment of origins of replication to the nuclear matrix and the chromosomal scaffold. *FEBS Lett* 1984;171:13–6. [PubMed: 6723972]
6. Razin S, Kekelidze MG, Lukanidin EM, Scherrer K, Georgiev GP. Replication origins are attached to the nuclear skeleton. *Nucleic Acids Res* 1986;14:8189–207. [PubMed: 3774556]
7. Dijkwel P, Wenink PW, Poddighe J. Permanent attachment of replication origins to the nuclear matrix in BHK-cells. *Nucleic Acids Res* 1986;14:3241–9. [PubMed: 3703674]
8. Pemov A, Bavykin S, Hamlin JL. Attachment to the nuclear matrix mediates specific alterations in chromatin structure. *Proc Natl Acad Sci USA* 1998;95:14757–62. [PubMed: 9843962]
9. Bode J, Benham C, Knopp A, Mielke C. Transcriptional augmentation: modulation of gene expression by scaffold/matrix-attached regions (S/MAR elements). *Crit Rev Eukaryot Gene Expr* 2000;10:73–90. [PubMed: 10813396]
10. Jackson D, Dickinson P, Cook PR. The size of chromatin loops in HeLa Cells. *EMBO J* 1990;9:567–71. [PubMed: 2303042]
11. Zink D. The temporal program of DNA replication: new insights into old questions. *Chromosoma* 2006;115:273–87. [PubMed: 16552593]
12. Nakamura H, Morita T, Sato C. Structural organizations of replicon domains during DNA synthetic phase in the mammalian nucleus. *Exp Cell Res* 1986;165:291–7. [PubMed: 3720850]
13. Nakayasu H, Berezney R. Mapping replication sites in the eucaryotic cell nucleus. *J Cell Biol* 1989;108:1–11. [PubMed: 2910875]
14. Mills A, Blow JJ, White JG, Amos WB, Wilcock D, Laskey RA. Replication occurs at discrete foci spaced throughout nuclei replicating in vitro. *J Cell Sci* 1989;94:471–7. [PubMed: 2632579]
15. Hozak P, Hassan AB, Jackson DA, Cook PR. Visualization of replication factories attached to nucleoskeleton. *Cell* 1993;73:361–73. [PubMed: 8097433]
16. Manders E, Stap J, Brakenhoff GJ, van Driel R, Aten JA. Dynamics of three-dimensional replication patterns during S-phase, analysed by double labelling of DNA and confocal microscopy. *J Cell Sci* 1992;103:857–62. [PubMed: 1478975]
17. Ma H, Samarabandu J, Devdhar RS, Acharya R, Cheng P-C, Meng C, et al. Spatial and temporal dynamics of DNA replication sites in mammalian cells. *J Cell Biol* 1998;143:1415–25. [PubMed: 9852140]
18. Hozak P, Cook PR. Replication factories. *Trends Cell Biol* 1994;4:48–52. [PubMed: 14731866]
19. Cook P. The organization of replication and transcription. *Science* 1999;284:1790–5. [PubMed: 10364545]
20. Holmquist G. Chromosome bands, their chromatin flavors, and their functional features. *Am J Hum Genet* 1992;51:17–37. [PubMed: 1609794]
21. Cohen SM, Furey TS, Doggett NA, Kaufman DG. Genome-wide sequence and functional analysis of early replicating DNA in normal human fibroblasts. *BMC Genomics* 2006;7:301. [PubMed: 17134498]
22. Saccone S, Caccio S, Kusuda J, Andreozzi L, Bernardi G. Identification of the gene-richest bands in human chromosomes. *Gene* 1996;174:85–94. [PubMed: 8863733]
23. Federico C, Saccone S, Bernardi G. The gene-richest bands of human chromosomes replicate at the onset of the S-phase. *Cytogenet Cell Genet* 1998;80:83–8. [PubMed: 9678339]
24. Sadoni N, Langer S, Fauth C, Bernardi G, Cremer T, Turner BM, et al. Nuclear organization of mammalian genomes: polar chromosome territories build up functionally distinct higher order compartments. *J Cell Biol* 1999;146:1211–26. [PubMed: 10491386]
25. Camargo M, Cervenka J. Patterns of DNA replication of human chromosomes. II. Replication map and replication model. *Am J Hum Genet* 1982;34:757–80. [PubMed: 7124731]
26. Holmquist G, Gray M, Porter T, Jordan J. Characterization of Geimsa dark- and light-band DNA. *Cell* 1982;31:121–9. [PubMed: 7159923]
27. Saitoh YLU. Metaphase chromosome structure: bands arise from a differential folding path of the highly AT-rich scaffold. *Cell* 1994;76:609–22. [PubMed: 7510215]
28. Huberman J, Riggs AD. Autoradiography of chromosomal DNA fibers from Chinese hamster cells. *Proc Natl Acad Sci USA* 1966;55:599–606. [PubMed: 5221245]



29. Merrick CJ, Jackson D, Diffley JF. Visualization of altered replication dynamics after DNA damage in human cells. *J Biol Chem* 2004;279:20067–75. [PubMed: 14982920]
30. Jackson DA, Pombo A. Replicon clusters are stable units of chromosome structure: evidence that nuclear organization contributes to the efficient activation and propagation of S phase in human cells. *J Cell Biol* 1998;140:1285–95. [PubMed: 9508763]
31. Daboussi R, Courbet S, Benhamou S, Kannouche P, Zdzienicka MZ, Debatisse, et al. A homologous recombination defect affects replication-fork progression in mammalian cells. *J Cell Sci* 2008;121:162–6. [PubMed: 18089650]
32. Frum R, Chastain PD 2nd, Qu P, Cohen SM, Kaufman DG. DNA replication in early S phase pauses near newly activated origins. *Cell Cycle* 2008;7:1440–8. [PubMed: 18418075]
33. Lebofsky R, Heilig R, Sonnleitner M, Weissenbach J, Bensimon A. DNA replication origin interference increases the spacing between initiation events in human cells. *Mol Cell Biol* 2006;17:5337–45.
34. Courbet S, Gay S, Arnoult N, Wronka G, Anglana M, Brison O, et al. Replication fork movement sets chromatin loop size and origin choice in mammalian cells. *Nature* 2008;455:557–60. [PubMed: 18716622]
35. Martin R, Oppenheim A. Initiation points for DNA replication in nontransformed and simian virus 40-transformed chinese hamster lung cells. *Cell* 1977;11:859–69. [PubMed: 196764]
36. Woodfine K, Fiegler H, Beare DM, Collins JE, McCann OT, Young BD, et al. Replication timing of the human genome. *Hum Mol Genet* 2004;13:191–202. [PubMed: 14645202]
37. Jeon Y, Bekiranov S, Karnani N, Kapranov P, Ghosh S, MacAlpine D, Lee C, et al. Temporal profile of replication of human chromosomes. *Proc Natl Acad Sci USA* 2005;102:6419–24. [PubMed: 15845769]
38. Zink D, Bornfleth H, Visser A, Cremer C, Cremer T. Organization of early and late replicating DNA in human chromosome territories. *Exp Cell Res* 1999;247:176–88. [PubMed: 10047460]
39. Kennedy BK, Barbie DA, Classon M, Dyson N, Harlow E. Nuclear organization of DNA replication in primary mammalian cells. *Genes Dev* 2000;14:2855–2868. [PubMed: 11090133]
40. Dimitrova D, Berezney R. The spatio-temporal organization of DNA replication sites is identical in primary, immortalized and transformed mammalian cells. *J Cell Sci* 2002;115:4037–51. [PubMed: 12356909]
41. Panning MM, Gilbert DM. Spatio-temporal organization of DNA replication in murine embryonic stem, primary, and immortalized cells. *J. Cell Biochem* 2005;95:74–82. [PubMed: 15723284]
42. Oppenheim A, Martin RG. Initiation points for DNA replication in nontransformed and simian virus 40-transformed BALB/c 3T3 cells. *J Virology* 1978;25:450–2. [PubMed: 202755]
43. Cohen SM, Cobb ER, Cordeiro-Stone M, Kaufman DG. Identification of chromosomal bands replicating early in the S phase of normal human fibroblasts. *Exp. Cell Res* 1998;245:321–9. [PubMed: 9851873]
44. Cha R, Kleckner N. ATR homolog Mec1 promotes fork progression, thus averting breaks in replication slow zones. *Science* 2002;297:602–6. [PubMed: 12142538]
45. Le Beau M, Rassool FV, Neilly ME, Espinosa R 3rd, Glover TW, Smith DI, et al. Replication of a common fragile site, FRA3B, occurs late in S phase and is delayed further upon induction: implications for the mechanism of fragile site induction. *Hum Mol Genet* 1998;7:755–61. [PubMed: 9499431]
46. Wang L, Darling L, Zhang J-S, Huang H, Liu W, Smith DI. Allele-specific late replication and fragility of the most active common fragile site, FRA3B. *Hum Mol Genet* 1999;8:431–7. [PubMed: 9949202]
47. Subramanian P, Nelson DL, Chinault AC. Large domains of apparent delayed replication timing associated with triplet repeat expansion at FRAXA and FRAXE. *Am J Hum Genet* 1996;59:407–16. [PubMed: 8755928]
48. Hansen R, Canfield TK, Fjeld AD, Mumm S, Laird CD, Gartler SM. A variable domain of delayed replication in FRAXA fragile X chromosomes: X inactivation-like spread of late replication. *Proc Natl Acad Sci USA* 1997;94:4587–92. [PubMed: 9114034]
49. Hellman A, Rahat A, Scherer SW, Darvasi A, Tsui LC, Kerem B. Replication delay along FRA7H, a common fragile site on human chromosome 7, leads to chromosomal instability. *Mol Cell Biol* 2000;20:4420–7. [PubMed: 10825205]

50. Hellman A, Zlotorynski E, Scherer SX, Cheung J, Vincent JB, Smith DI, et al. A role for common fragile site induction in amplification of human oncogenes. *Cancer Cell* 2002;1:89–97. [PubMed: 12086891]
51. Brylawski BP, Chastain PD 2nd, Cohen SM, Cordeiro-Stone M, Kaufman DG. Mapping of an origin of DNA replication in the promoter of fragile X gene FMR1. *Exp Mol Pathol* 2007;82:190–6. [PubMed: 17196195]
52. Chastain PD 2nd, Cohen SM, Brylawski BP, Cordeiro-Stone M, Kaufman DG. A late origin of DNA replication in the trinucleotide repeat region of the human FMR2 gene. *Cell Cycle* 2006;5:869–72. [PubMed: 16582587]
53. Conti C, Sacca B, Herrick J, Lalou C, Pommier Y, et al. Replication fork velocities at adjacent replication origins are coordinately modified during DNA replication in human cells. *Mol Biol Cell* 2007;18:3059–3067. [PubMed: 17522385]
54. Huberman JA, Riggs AD. On the mechanism of DNA replication in mammalian chromosomes. *J Mol Biol* 1968;32:327–41. [PubMed: 5689363]
55. Berezney R, Dubey DD, Huberman JA. Heterogeneity of eukaryotic replicons, replicon clusters, and replication foci. *Chromosoma* 2000;108:471–84. [PubMed: 10794569]
56. Cejpek E, Tsai M-J, O'Malley BW. Actively transcribed genes are associated with the nuclear matrix. *Nature* 1983;306:607–9. [PubMed: 6646237]
57. Rose S, Garrard WT. Differentiation-dependent chromatin alterations precede and accompany transcription of immunoglobulin light chain genes. *J Biol Chem* 1984;259:8534–44. [PubMed: 6429143]
58. Small D, Nelkin B, Vogelstein B. The association of transcribed genes with the nuclear matrix of *Drosophila* cells during heat shock. *Nucleic Acids Res* 1985;13:2413–31. [PubMed: 2987852]
59. Birch H, Schreiber G. The association of acute phase protein genes with the nuclear matrix of rat liver during experimental inflammation. *Biochem Biophys Res Commun* 1986;137:633–9. [PubMed: 2425799]
60. Stratling W. Gene-specific differences in the supranucleosomal organization of rat liver chromatin. *Biochemistry* 1987;26:7893–9. [PubMed: 2447949]
61. Delcuve G, Davie JR. Chromatin structure of erythroid-specific genes of immature and mature chicken erythrocytes. *Biochem J* 1989;263:179–86. [PubMed: 2604693]
62. Ogata N. Preferential association of a transcriptionally active gene with the nuclear matrix of rat fibroblasts transformed by a simian-virus-40-pBR322 recombinant plasmid. *Biochem J* 1990;267:385–90. [PubMed: 2159279]
63. Deuring R, Fanti L, Armstrong JA, Sarte M, Papoulas O, Prestel M, et al. The ISWI chromatin-remodeling protein is required for gene expression and the maintenance of higher order chromatin structure in vivo. *Mol Cell* 2000;5:355–65. [PubMed: 10882076]
64. Friedman K, Diller JD, Ferguson BM, Nyland SV, Brewer BJ, Fangman WL. Multiple determinants controlling activation of yeast replication origins late in S phase. *Genes Dev* 1996;10:1595–607. [PubMed: 8682291]
65. Kornberg R, Lorch Y. Interplay between chromatin structure and transcription. *Curr Opin Cell Biol* 1995;7:371–5. [PubMed: 7662367]
66. Leach T, Chotkowski HL, Wotring MG, Dilwith RL, Glaser RL. Replication of heterochromatin and structure of polytene chromosomes. *Mol Cell Biol* 2000;20:6308–16. [PubMed: 10938107]
67. Tomilin NSL, Krutilina R, Chamberland C, Hancock R, Vig B. Visualization of elementary DNA replication units in human nuclei corresponding in size to DNA loop domains. *Chromosome Research* 1995;3:32–40.
68. Micheli G, Luzzatto AR, Carri MT, de Capoa A, Pelliccia F. Chromosome length and DNA loop size during early embryonic development of *Xenopus laevis*. *Chromosoma* 1993;102:478–83. [PubMed: 8375216]
69. Linskens M, Eijsermans A, Dijkwel PA. Comparative analysis of DNA loop length in nontransformed and transformed hamster cells. *Mut Res* 1987;178:245–56. [PubMed: 3587255]
70. Demeret C, Vassetzky Y, Mechali M. Chromatin remodelling and DNA replication: from nucleosomes to loop domains. *Oncogene* 2001;20:3986–093. [PubMed: 11494127]

71. Buongiorno-Nardelli M, Micheli G, Carri MT, Marilley M. A relationship between replicon size and supercoiled loop domains in the eukaryotic genome. *Nature* 1982;298:100–2. [PubMed: 7088157]
72. Marilley M, Gassend-Bonnet G. Supercoiled loop organization of genomic DNA: a close relationship between loop domains, expression units, and replicon organization in rDNA from *Xenopus laevis*. *Exp Cell Res* 1989;180:475–89. [PubMed: 2536612]
73. Heffernan TP, Simpson DA, Frank AR, Heinloth AN, Paules RS, Cordeiro-Stone M, et al. An ATR- and Chk1-dependent S checkpoint inhibits replicon initiation following UVC-induced DNA damage. *Mol Cell Biol* 2002;22:8552–61. [PubMed: 12446774]
74. Boyer JC, Kaufmann WK, Cordeiro-Stone M. Role of postreplication repair in transformation of human fibroblasts to anchorage independence. *Cancer Research* 1991;51:2960–4. [PubMed: 1903328]
75. Parra I, Windle B. High resolution visual mapping of stretched DNA by fluorescent hybridization. *Nat Genet* 1993;5:17–21. [PubMed: 8106079]
76. White AE, Livanos EM, Tlsty TD. Differential disruption of genomic integrity and cell cycle regulation in normal human fibroblasts by the HPV oncoproteins. *Genes Dev* 1994;8:666–77. [PubMed: 7926757]

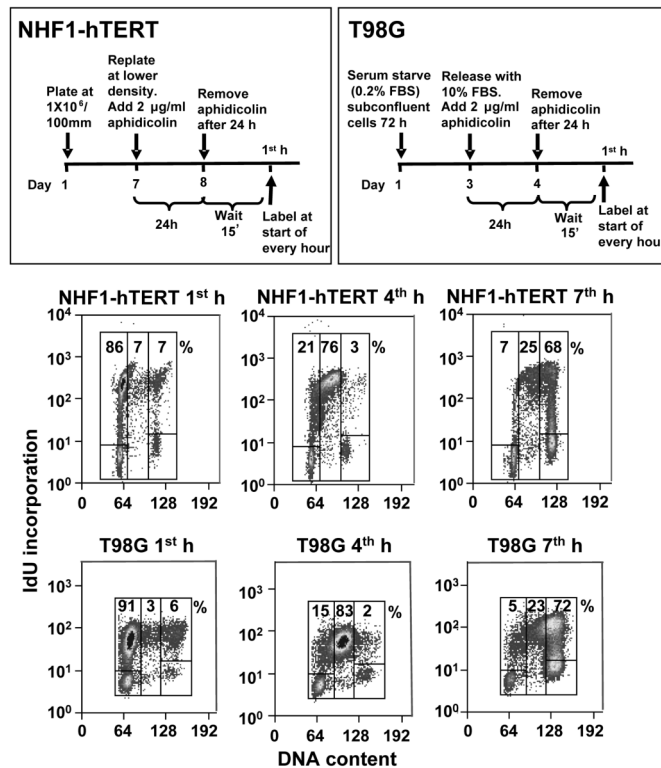


**Figure 1. Synchronous progression of NHF1-hTERT and T98G cells through the S phase**  
 NHF1-hTERT cells were plated at  $10^6$  cells/100mm plate and were grown to confluence. On the seventh day, the cells were replated at a lower density to enable them to re-enter the cell cycle in the presence of 2  $\mu\text{g/ml}$  aphidicolin. After 24 hours, aphidicolin was removed, and cells were given a 15 minute recovery time; thereafter cells were labeled for 10 minutes with IdU followed by 20 minutes with CldU at the start of every hour for 7 hours. Similarly, subconfluent T98G cells were synchronized by 0.2% serum starvation for 72 hour, followed by release with 10% serum in the presence of aphidicolin. After 24 hours, aphidicolin was removed, and after a 15 minute recovery period, cells were labeled as for NHF1-hTERT cells, at the start of every hour for 7 hours. Synchronous progression of NHF1-hTERT and T98G cells is shown for early, mid and late S phase time-points. Both cell lines showed a similar distribution of early, mid and late S phase cells during the 1<sup>st</sup>, 4<sup>th</sup> and 7<sup>th</sup> hours after removal of aphidicolin.

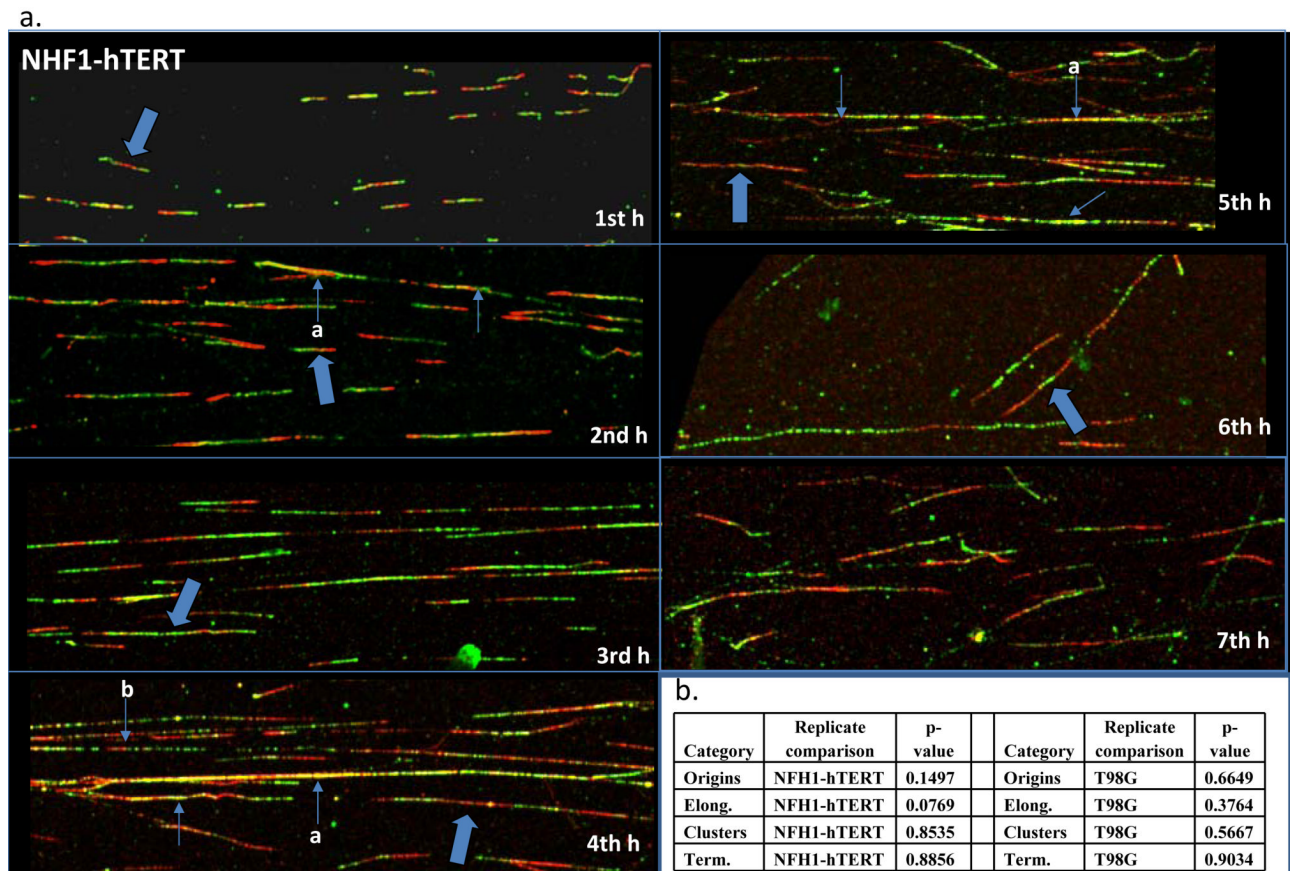


### Figure 2. Fiber analysis of replicating DNA in NHF1-hTERT cells

(a) A snapshot of typical replication patterns observed in NHF1-hTERT cells at the start of every hour of S phase after 10 minute labeling with IdU (red) followed by 20 minute labeling with CldU (green). Fibers were included in the analysis when they contained red and green tracks that were clearly stained in a way that the tracks could be distinguished from each other and where fibers to be scored were not tangled with other fibers that would interfere with the interpretation of their labeling pattern. The block arrows identify examples of fibers that would be counted in the study, although similar scorable fibers are also clearly present in the images: single bidirectional origins (1<sup>st</sup> hour), unidirectional elongation (2<sup>nd</sup> hour), clusters (3<sup>rd</sup> and 4<sup>th</sup> hours) and terminations (5<sup>th</sup> and 6<sup>th</sup> hours) are shown. Only labeled fibers whose entire lengths were contained in the images were counted in the analysis. Examples of labeled fibers that would not be counted in the study are shown by small arrows. Exclusion of fibers from the study resulted from factors such as tangling with other labeled fibers (small arrows labeled “a” in 2<sup>nd</sup>, 4<sup>th</sup> and 5<sup>th</sup> hours) or excessive spottiness of staining (small arrows labeled “b” in 4<sup>th</sup> hour) that made interpretation of the patterns difficult. Yellow color in the fibers is a result of overlap between the red and green stains; this can occur as a result of staining with the antibodies at intersections between the red and green labels, or by overlapping fibers, or a result of cross-reactivity of the antibodies or re-replication. Fibers with spots of yellow were included in the analysis if the yellow color did not interfere with interpretation of the patterns (block arrows in 3<sup>rd</sup> and 4<sup>th</sup> hours). (b) Statistical reproducibility between replicates of NHF1-hTERT or T98G cells are shown with p-values higher than 0.05. The percentages of each category (origins, elongations, clusters or terminations) for the entire S phase were compared between replicates of the same cell line. For the entire S phase, all categories showed statistical similarity between replicates of the same cell line, suggesting reproducibility between replicates.

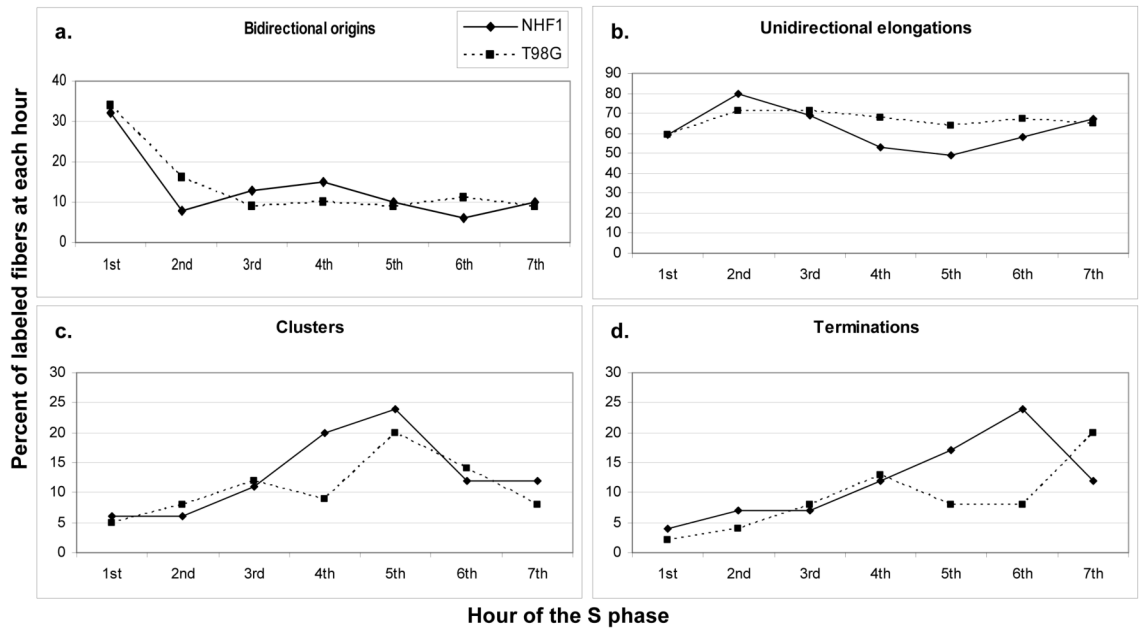


**Figure 3. Percent distribution of labeled replication patterns in NHF1-hTERT and T98G cells at every hour for 7 hours of S phase**

The labeled tracks of replicating DNA in fiber spreads were counted and divided into categories of single bidirectional origins (a), unidirectional elongations (b), clusters (c) and terminations (d). The percent of fibers in all four categories at every hour equals 100%.

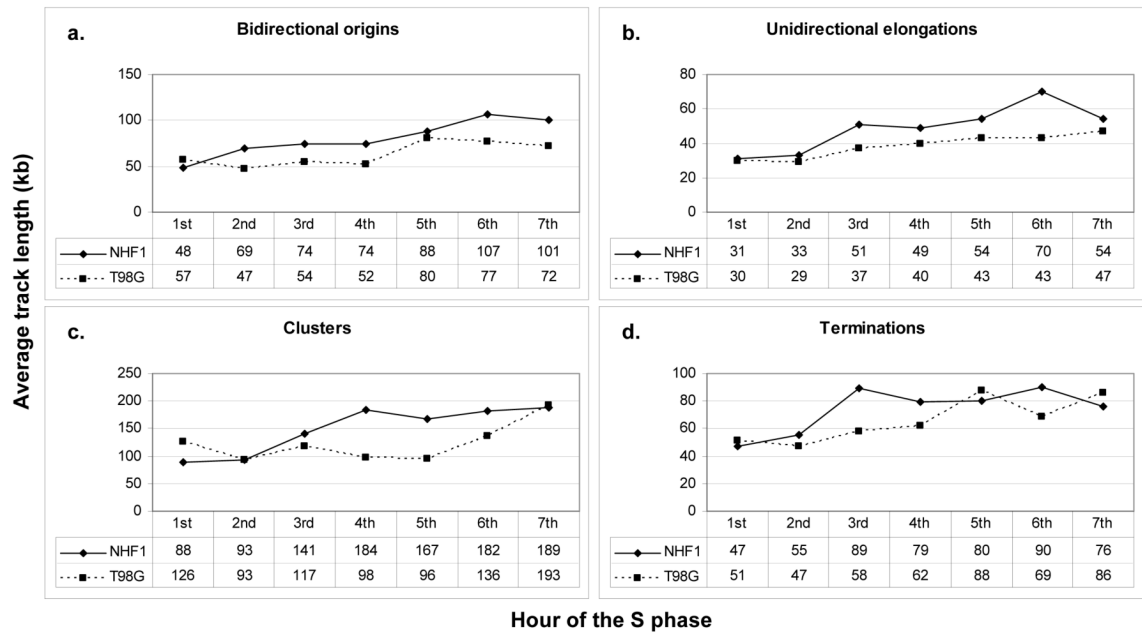


**Figure 4. Comparison of average track lengths of single bidirectional origins, unidirectional elongations, clusters and terminations in NHF1-hTERT and T98G cells at every hour for 7 hours of S phase**

The average length of replicating DNA in fiber spreads were measured and divided into categories of single bidirectional origins (a), unidirectional elongations (b), clusters (c), and terminations (d), for the start of every hour of S phase for both NHF1-hTERT and T98G cells. The arbitrary length of measurement was converted into kb using the conversion factor 867.5 base pairs/arbitrary unit.<sup>32</sup> The lengths in kb are shown and indicated below the chart for every hour in both NHF1-hTERT and T98G cells.

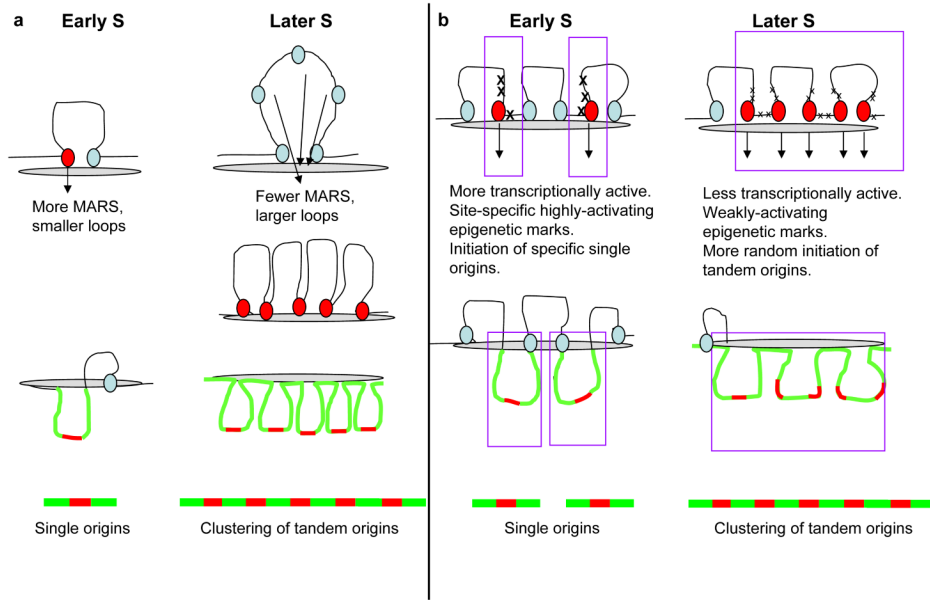


**Figure 5. Proposed models for organization of DNA into single bidirectional origins or clusters**

**(a)** DNA is thought to be organized into loops through attachment of the DNA to the nuclear matrix at matrix attachment regions (MARS) located near origins. DNA that replicates in early S phase is enriched in genes that are actively transcribed in the cell. Since actively transcribed genes have been shown to be enriched in MARS, it is expected that there is more attachment of early replicating DNA to the matrix, potentially creating smaller loops with fewer origins. We propose that when these loops are reeled through replication factories at the matrix, the paucity of origins per loops results in an enrichment of the non-clustered bidirectional origin replication patterns that we observe in the early S phase of NHF1-hTERT and T98G cells. However, sequences that replicate later in S phase are generally gene-poor. It is therefore expected that there are fewer sites of attachment of the DNA to the matrix during mid S phase, resulting in larger loops with potentially more origins per loop. When these mid S phase loops are reeled through replication factories at the matrix, we hypothesize the larger number of origins per loop assemble at the replication factories at the matrix and simultaneously fire. This could result in the clustered pattern of tandem-firing replicons that we typically observe in mid S phase in NHF1-hTERT cells. **(b)** An alternate model suggests that the way origins are epigenetically marked in early and later S phase determines the way they get replicated. The alternate model is based on the findings that DNA that replicates in early S phase is more transcriptionally active and contains more site-specific highly-activating epigenetic marks. This would lead to initiations of specific single origins that we observe in early S phase. However, DNA replicated later in S phase is less transcriptionally active and may contain more weakly-activating epigenetic marks. This may lead to more random initiation of tandem origins, and simultaneous firing of adjacent origins found in clusters during mid to late S phase.



**Table 1**  
**Comparison of percent distribution of replication patterns by hour and category in NHF1-hTERT and T98G cells**

Percent distributions are presented in columns for single bidirectional origins, unidirectional elongations, clusters and terminations present for each of the 7 hours of S phase for T98G or NHF1-hTERT cells. The percents of all four categories at each hour equals 100%. The percents of each category at every hour were compared between the cell lines for statistical significance. The p-value for this comparison is shown in the far right column for every category. Significant differences indicated by a p-value of 0.05 or less are shown in bold.

Category	Hour	T98G %	NHF1-hTERT %	p-value
bidir. origins	1st	34.4	31.7	0.4976
bidir. origins	2nd	16.5	8.0	<b>0.0155</b>
bidir. origins	3rd	9.5	13.3	0.2764
bidir. origins	4th	10.4	14.7	0.2164
bidir. origins	5th	9.2	10.0	0.8390
bidir. origins	6th	11.3	6.0	0.1291
bidir. origins	7th	8.5	9.6	0.7563
unidir. elong.	1st	58.5	59.1	0.8962
unidir. elong.	2nd	71.2	79.9	<b>0.0131</b>
unidir. elong.	3rd	70.7	69.1	0.6577
unidir. elong.	4th	67.5	53.1	<b>&lt;.0001</b>
unidir. elong.	5th	63.6	48.7	<b>&lt;.0001</b>
unidir. elong.	6th	66.7	57.7	<b>0.0102</b>
unidir. elong.	7th	64.5	66.5	0.5695
clusters	1st	5.4	5.7	0.9312
clusters	2nd	8.4	5.5	0.4185
clusters	3rd	11.8	10.8	0.7820
clusters	4th	9.3	19.9	<b>0.0026</b>
clusters	5th	19.6	24.4	0.1736
clusters	6th	14.4	12.5	0.5888
clusters	7th	7.50	12.3	0.1724
term.	1st	1.7	3.6	0.6444
term.	2nd	4.0	6.6	0.4535
term.	3rd	8.0	6.7	0.7124
term.	4th	12.8	12.2	0.8655
term.	5th	7.6	17.0	<b>0.0078</b>
term.	6th	7.6	23.9	<b>&lt;.0001</b>
term.	7th	19.5	11.6	<b>0.0248</b>

**Table 2**  
**Statistical significance of changes between successive hours of S phase in the percent distributions of bidirectional origins, unidirectional elongations, clusters and terminations**

The percents of single bidirectional origins, unidirectional elongations, clusters, and merging forks (terminations) were individually compared hour by hour between subsequent hours for the same cell line to determine their statistical significance. The p-values for all four categories are shown for each hourly transition throughout S phase in both NHF1-hTERT and T98G cells. Significant differences within the same category as S phase progresses hour to hour within the same cell line are indicated by a p-value of 0.05 or less. These p-values correspond to the changes in percent distributions illustrated in Figure 3. An hour-to-hour comparison for all hours of S phase for both cell lines is shown in Supplemental Table 1.

NHF1-hTERT				
Hours compared	Bidirectional origins p-value	Unidirectional elongations p-value	Clusters p-value	Merging forks (terminations) p-value
1 to 2	<b>0.0001</b>	< <b>0.0001</b>	0.9583	0.3448
2 to 3	0.1275	<b>0.0022</b>	0.1318	0.9758
3 to 4	0.6904	< <b>0.0001</b>	<b>0.0100</b>	0.1151
4 to 5	0.1755	0.2092	0.2052	0.1791
5 to 6	0.2614	<b>0.0110</b>	<b>0.0007</b>	<b>0.0497</b>
6 to 7	0.3076	<b>0.0121</b>	0.9649	<b>0.0005</b>

T98G				
Hours compared	Bidirectional origins p-value	Unidirectional elongations p-value	Clusters p-value	Merging forks (terminations) p-value
1 to 2	<b>0.0001</b>	<b>0.0034</b>	0.4831	0.5969
2 to 3	<b>0.0471</b>	0.8907	0.3297	0.2508
3 to 4	0.8020	0.3634	0.4725	0.1686
4 to 5	0.7477	0.2651	<b>0.0035</b>	0.1370
5 to 6	0.5501	0.3755	0.1386	0.9976
6 to 7	0.4192	0.5309	0.0513	<b>0.0007</b>

**Table 3**  
**Comparison of replication track lengths by hour and category between NHF1-hTERT and T98G cells**

The average lengths of labeled tracks (in arbitrary units) of replicating single bidirectional origins, unidirectional elongations, clusters and terminations produced during the 30 min total labeling period in NHF1-hTERT or T98G cells were compared between cell lines by category at every hour. The average red+green track lengths of each of the four categories is shown at each hour for both T98G and NHF1-hTERT cells. A statistical analysis was performed for each category by hour between cell lines, and the p-value shows statistical similarities and differences in the lengths of replication DNA tracks in the two cell lines. Significant differences indicated by a p-value of 0.05 or less between cell lines are shown in bold in the right-hand column.

Category	Period (hour)	T98G (Arbitrary units)	NHF1-hTERT (Arbitrary units)	p-value
bidir. origins	1st	66.5	54.7	0.0323
bidir. origins	2nd	54.4	79.0	0.0114
bidir. origins	3rd	61.8	85.0	0.0142
bidir. origins	4th	60.4	85.4	0.0062
bidir. origins	5th	92.1	101.6	0.4436
bidir. origins	6th	89.4	123.0	0.0054
bidir. origins	7th	82.8	115.7	0.0100
unidir. elong.	1st	34.9	35.6	0.8568
unidir. elong.	2nd	34.1	37.7	0.3212
unidir. elong.	3rd	42.8	58.6	<.0001
unidir. elong.	4th	45.8	57.0	0.0078
unidir. elong.	5th	48.5	61.7	0.0091
unidir. elong.	6th	48.7	80.5	<.0001
unidir. elong.	7th	54.2	61.7	0.1138
clusters	1st	145.5	101.4	0.0010
clusters	2nd	106.9	106.7	0.9888
clusters	3rd	135.3	161.7	0.0047
clusters	4th	112.8	211.8	<.0001
clusters	5th	110.8	191.7	<.0001
clusters	6th	156.5	209.7	<.0001
clusters	7th	222.5	217.8	0.7072
term.	1st	58.6	54.3	0.8179
term.	2nd	54.2	62.9	0.6086
term.	3rd	67.3	102.5	0.0027
term.	4th	72.4	90.6	0.0497
term.	5th	101.0	91.7	0.4893
term.	6th	80.3	104.1	0.0203
term.	7th	99.0	88.0	0.3225

**Table 4**  
**Comparison of replication track lengths by category or hour for the averaged S phase of NHF1-hTERT and T98G cells**

The track lengths of replicating DNA in NHF1-hTERT and T98G cells were compared between cell lines as (a) an average by category for the entire S phase or (b) as an average of all replicating tracks by hour throughout S phase. A statistical analysis was performed to determine differences between cell lines. Significant differences indicated by a p-value of 0.05 or less between cell lines are shown in bold in the right-hand column.

<b>a</b>			
<b>Category</b>	<b>T98G (Arbitrary Units)</b>	<b>NHF1- hTERT (Arbitrary units)</b>	<b>p-value</b>
clusters	141.5	171.5	<.0001
unidir. elong.	44.1	56.1	<.0001
bidir. origins	72.5	92.1	<.0001
terminations	76.1	84.9	0.0844

<b>b</b>			
<b>Period (hour)</b>	<b>T98G (Arbitrary Units)</b>	<b>NHF1- hTERT (Arbitrary units)</b>	<b>p-value</b>
1st	76.3	61.5	0.0128
2nd	62.4	71.6	0.1156
3rd	76.8	101.9	<.0001
4th	72.9	111.2	<.0001
5th	88.1	111.7	<.0001
6th	93.7	129.3	<.0001
7th	114.6	120.8	0.2520

Table 5

## Average number of red tracks (origins) in a cluster

To determine the average inter-origin distance in a cluster (represented by red tracks within clusters), we counted the number of red tracks in all clusters at each hour and divided this averaged number into the average length of clusters (converted to kb as described in Methods) at that hour. The average number of red tracks in a cluster is shown by hour as well as an average throughout S phase for both NHF1-hTERT and T98G cells. Also shown is the average distance between red tracks (kb) by hour for both cell lines.

Hour	Avg number of red tracks in clusters		Statistical significance of percent distributions	Statistical significance of lengths	Avg distance (kb) between red tracks		Fold diff.
	NHF1-hTERT	T98G			NHF1-hTERT	T98G	
1 <sup>st</sup>	2.2	2.4	Same	T98G longer	40	53	0.75
2 <sup>nd</sup>	2.3	2.3	Same	Same	40	40	1.0
3 <sup>rd</sup>	2.5	2.5	Same	T98G shorter	56	47	1.2
4 <sup>th</sup>	3.1	2.5	Fewer in T98G	T98G shorter	59	39	1.5
5 <sup>th</sup>	2.6	3.1	Same	T98G shorter	64	31	2.1
6 <sup>th</sup>	2.5	2.4	Same	T98G shorter	73	57	1.3
7 <sup>th</sup>	2.8	2.9	Same	Same	68	67	1.0
Avg.	2.6	2.6	-	-	57	48	-